International Journal of Sustainable Energy and Environmental Research
2019 Vol. 8, No. 1, pp. 48-61
ISSN(e): 2306-6253
ISSN(p): 2312-5764
DOI: 10.18488/journal.13.2019.81.48.61

OPTIMAL DESIGN OF HYBRID ENERGY SYSTEM DRIVES SMALL-SCALE REVERSE OSMOSIS DESALINATION PLANT

M. Osman[1+]
M. A. Farahat[2]
Mohammed Elsayed Lotfy[3]

[1,2]Electrical Power & Machines Department, Zagazig University, Zagazig, 44519, Egypt
[1]Email: m.aatallah@zu.edu.eg
[2]Email: mamfarahat59@gmail.com
[3]Electrical Power & Machines Department, Zagazig University, Zagazig, 44519, Egypt & Department of Electrical and Electronics Engineering, Ryukyus University, Okinawa, 903-0213, Japan
[3]Email: mohamedabozed@zu.edu.eg

(+ Corresponding author)

Article History
Received: 14 November 2018
Revised: 18 December 2018
Accepted: 24 January 2019
Published: 11 March 2019

Keywords
Freshwater
Nakhl
Hybrid
Cycle cost
Homer Pro
Reverse osmosis
Renewable.

ABSTRACT

Different configurations for a hybrid energy system are presented. This study aims to produce 100 m^3/day of freshwater for 120,000 people at Nakhl city, North Sinai, Egypt. This simulation selects the optimal design of the hybrid energy system according to the net present cost (NPC), the cost of energy (COE), the gases emissions (carbon dioxide, sulfur dioxide) and the excess system electricity. The hybrid system consists of photovoltaic panels, wind turbines, storage batteries, and a diesel generator. The operation of five different systems is studied to supply the load at an average rate of 557.22 kWh/day with 35.67 kW peak load. In order to minimize the system total cycle cost, both of the photovoltaic modules sizing, the wind turbine production, the number of battery strings and the diesel generator fuel consumption are studied. Homer Pro software is used to select the optimal system configuration. The results illustrate that the hybrid PV/diesel/RO desalination plant system with storage batteries is sustainable and socially accepted system. It consists of 83.5 kW PV panels, a 36.4 kW converter, seven strings of lead-acid batteries and a 50 kW fixed capacity generator. Also, the system achieves the lowest cost of energy and net present cost.

Contribution/Originality: This study is one of very few studies which have investigated the optimal hybrid power system configuration to drive a reverse osmosis desalination plant at the Nakhl city, Egypt. This study documents that renewable energy is the effective option to face the fuel energy pollution by reducing the gases emissions from burning fossil fuels.

NOMENCLATURE

NPC	Net present cost	CO2	Carbon dioxide
COE	Cost of energy	PV	Photovoltaic
RO	Reverse osmosis	STC	Standard test condition
HP	High-pressure pump	RES	Renewable energy supply

1. INTRODUCTION

Renewable energy is a useful option to face fuel energy pollution (Talaat *et al.*, 2016). Also, arid and remote areas suffer from the lack of freshwater and no electrical grid connections due to their geographic location (Ahmed *et al.*, 2019). So, reverse osmosis (RO) desalination plant powered by hybrid energy sources can solve the shortage of clean water in remote and arid areas. Also, the fuel energy participation percentage will be decreased which reduces the percentage of gases emissions. Abdel-karim Daud et al. conducted a study to meet the residential load demand in Palestine (Daud and Ismail, 2012). The results showed that the hybrid PV/wind/battery/diesel system is the most economical system. It is a high reliability and efficiency system. Ahmed M.A. Haidar et al. studied the use of hybrid PV/wind/diesel system to choose the optimal configuration of a renewable energy system in Malaysia (Haidar *et al.*, 2011). The study is performed by Homer software. The results showed that PV/diesel system is the optimal solution in Malaysia. The system achieved a proper economic performance and low gas emissions.

Elizabeth Harder et al. performed research in a photovoltaic power plant in Abu Dhabi to examine the financial feasibility, production of energy and gases emissions using RETScreen software (Harder and Gibson, 2011). The system achieved high energy production, low gases emissions, and poor financial prospects. N. Phuangpornpitak et al. conducted a study at islanders community to check the effect of hybrid PV/diesel system on an island (Phuangpornpitak and Kumar, 2011). They concluded that the hybrid system is satisfactory compared to the diesel generator only. Assessment of the potential of renewables for Brunei Darussalam using RES and Homer software has been reported in Malik (2011). Luis Arriabs et al. suggested the guidelines for PV/wind hybrid system. They applied their suggestion to hybrid PV/wind system installed in (Soria, Spain) (Arribas *et al.*, 2010). The results showed that the wind technology presented higher performance than others.

A. Demiroren et al. conducted a study to examine the optimal system configuration of hybrid and non-hybrid renewable energy system in Turkey (Demiroren and Yilmaz, 2010). Homer software is used to make the proposed system as real as possible. The results showed that the wind energy costs are the lowest for Gökceada.

This paper studies five different scenarios, namely a stand-alone diesel generator system without a storage element, hybrid PV/diesel system with a storage element, hybrid wind/diesel system with a storage element, hybrid PV/wind system with a storage element and hybrid PV/wind/diesel system with a storage element. Solar radiation and wind speed data are taken from NASA (National Aeronautics and Space Administrative). Homer Pro (National Renewable Energy Laboratory, US) software is used to compute the optimal configuration of hybrid energy systems. This project is performed in Egypt with annual inflation rate equals 16%, and real discount rate equals 16.75% as referred in October 2018 (Trading Economics, 2018). The project lifetime is proposed to be 25 years.

2. METHODOLOGY

Homer Pro software uses some parameters to select the optimal hybrid system configuration. These parameters include site description, load profile, resources availability, system components and components cost. The following section discusses these parameters.

2.1. Site Description

The peninsula of Sinai enjoys a sunny atmosphere throughout the year and extreme winds, especially in the winter. So, the proposed system is established at Nakhl city, North Sinai governorate, Egypt as shown in Figure 1. This location is 420.6 m above sea level at longitude and latitude which equal 34 ° 17.1′ E and 29 °39.4′ N respectively. The city is characterized by large solar radiation and high wind speed due to its geographical location which is surrounded by mountains and hills.

2.2. Electrical Load Demand

The daily load profile of the proposed reverse osmosis desalination plant is shown in Figure 2. This plant consists of lighting loads, filter pump, high-pressure pumps (HP) and product water pump. The lighting loads consume 49.9 kWh of electricity per day which represents 8.9% of the total load. The dissolved solids are disposed of by a filter pump. This pump consumes 122.24 kWh of electricity per day which represents about 21.93% of the total consumption. Two high-pressure pumped consume 358.08 kWh/day which represents about 64.26% of the total load to separate the clean water. Finally, the potable water can be obtained through the product water pump. It operated for 5hrs/day and consumed 27 kWh of electricity per day which represents about 4.8% of the total load. So, the desalination plant consumes 557.22 kWh of electricity per day which equals 203.385 MWh of electricity per year. The technical specifications of the proposed RO desalination plant are listed in Table 1.

Figure-1. The proposed site from NASA (Nakhl city, North Sinai, Egypt).
Source: NASA (2018).

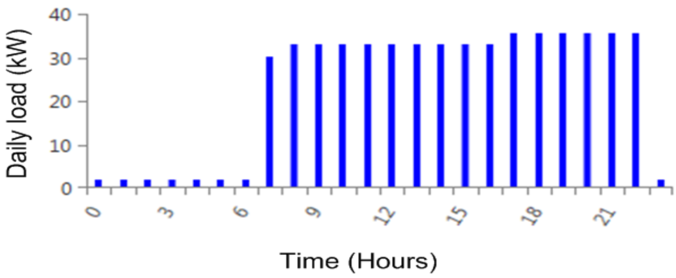

Figure-2. Daily load profile for the proposed RO desalination plant.
Source: Generated by the authors using HOMER Pro software.

2.3. Resources Significance and Availability

The process of linking renewable energy sources and desalination plants in remote areas is the most appropriate solution to eliminate water shortage problems (Mehdi *et al.*, 2014). Also, the renewable energy source is called clean energy and environmentally friendly for their useful role in reducing emissions from fossil fuels burning in the conventional sources (Ngan and Tan, 2012). The following section presents the solar radiation, wind speed and diesel fuel price at the proposed location.

Table-1. Technical specifications of the proposed RO desalination plant.

Characteristic	Unit	Value
Feed pressure	Bar	21
Pump efficiency	--	0.85
Feed flow	m^3/h	10
Permeate flow	m^3/h	100
Membrane manufacture	--	FILMTEC.-BW30-400
Membrane element numbers	--	6
Feed temperature	^oc	27 – 45
Feed pump consumption	kW	7.64
High-pressure Consumption	kW	22.38
Product water power consumption	kW	3
Lighting Loads	kW	7.65
Daily operating hours	hours	16

Source: (Reports, 2016, Datasheet).

2.3.1. Solar

Homer Pro software uses the solar data as an input parameter to select the optimum number of photovoltaic panels. These data are taken from NASA (NASA, 2018). Solar data are classified as solar radiation and clearness index. The clearness index shows the degree of fineness of the atmosphere from clouds (Gökçek, 2018). From Homer software, the clearness index ranges from zero to one (HOMER Energy, 2018). Figure 3 shows the annual average solar radiation and the clearness index at the Nakhl city, Egypt. At the proposed location, the solar radiation varies from 6.12 kWh/m^2/day at January to 9.81 kWh/m^2/day at September with annual average value equals 7.81 kWh/m^2/day. Also, the clearness index equals 0.66.

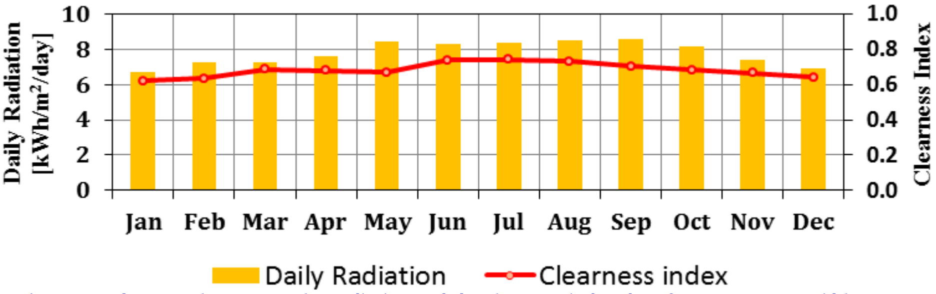

Figure-3. The annual average solar radiation and the clearness index data from NASA at Nakhl, Egypt.
Source: Generated by the authors from NASA (2018).

2.3.2. Wind

The wind turbine is one of the most important sources of renewable energy. About 35 million people worldwide rely on wind energy to meet 4% of the total global energy (Bansal *et al.*, 2005). Egypt is also seeking to achieve the highest wind production by about 12% in 2022. At the proposed site, the wind speed data are taken from NASA (2018). Homer software uses the wind speed data at 50 m above the earth surface in the simulation. Figure 4 shows the annual average wind speed at the Nakhl city. The lowest wind speed was recorded in November at about 2.27 m/s. However, the highest wind speed was recorded in January at about 12.78 m/s.

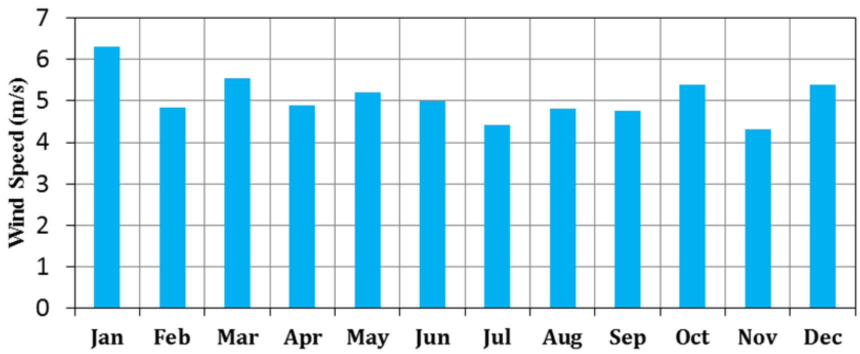

Figure-4. The annual average wind speed data from NASA at Nakhl, Egypt.
Source: Generated by the authors from NASA (2018).

2.3.3. Diesel

In this study, the diesel generator is used as a backup source to compensate for the shortage of electricity due to the failure of renewable energy sources. As a result of economic reform in Egypt, the price of petrol is continuously changing. The latest fuel price update is used for this research. It equals L.E 5.5/L or $ 0.31/L in 2019 (Global Petrol Prices, 2019).

2.4. System Description and Specification

Photovoltaic panels, wind turbines, and diesel generator are the main components of the proposed hybrid energy system. Also, power conditioning units and storage batteries are more detailed modeling to save the system stability and reliability. Table 2 illustrates the technical specifications, components description and parameters cost of the proposed power system at the Nakhl city.

2.4.1. Photovoltaic Modules

The following equation can express the output power of the photovoltaic modules:

$$P_{output-PV} = P_{rated-PV}\, F_{PV} \left(\frac{G_i}{G_{i-STC}}\right)\left[1 + \alpha_p (T_c - T_{c,STC})\right] \quad (1)$$

Table-2. Technical and economic specifications of the power system considered.

Description	Unit	Specification
PV modules		
PV model	--	Sharp ND-250QCS
Rated power	kW	0.250
Capital cost	$/kW	2000
Lifetime	years	25
Derating factor	%	88
Wind turbine		
Type of wind turbine	--	Xzeres 7.2
Rated power	kW	10
Capital cost	$/unit	50000
Lifetime	year	20
Diesel generator		
Generator model	---	Generic fixed capacity
Rated power	kW	50
Capital cost	$/kW	500
Lifetime	hours	15000
Diesel fuel price	$/L	0.31
Storage battery		
Type of battery	--	Trojan SAGM 12 205
Capital cost	$/unit	600
Lifetime	years	8+
Converter		
Converter model	--	Generic converter
Capital cost	$/kW	300
Lifetime	year	15
Conversion efficiency	%	95

Source: (CAPSELLS, 2018; GoGreenSolar, 2018; HOMER Energy, 2018; SOLARIS, 2018).

Where $P_{rated-PV}$ is the rated capacity of the photovoltaic system, F_{PV} (derating factor) is a percentage value which increases the PV system efficiency, G_i is the incident solar radiation on the working plane (W/m²), G_{i-STC} is the total solar radiation under stander test condition (STC), α_p is a percentage value of each Celsius degree (% / °c) which represents the power temperature coefficient, T_c is the photovoltaic module temperature (°c) and $T_{c,STC}$ is the photovoltaic module temperature under stander test condition (Ghenai *et al.*, 2018; Gökçek, 2018; HOMER Energy, 2018).

Sharp ND-250QCS photovoltaic module is used in this paper. This module consists of 60 polycrystalline silicon cells with 250 watts maximum power. The cells are connected in series (SHARP, 2018). The photovoltaic panels are designed with zero panel azimuth and 29.99 ° panel slope without a tracking system. The ambient temperature affects the output power of the photovoltaic modules (Li *et al.*, 2009; Nema *et al.*, 2009; Ngan and Tan, 2012). So, it should be taken into account. The temperature coefficient (I_{sc}) is 0.053% /°c, ($V_{o.c}$) is -0.36% /°c and (P_{max}) is 0.485% /°c. Table 3 presents the photovoltaic module characteristics.

Table-3. Technical characteristics of the Sharp ND-250QCS module.

Characteristics	Unit	Value
Maximum Power Voltage (V_{pm})	V	29.8
Open circuit voltage ($V_{o.c}$)	V	38.3
Maximum Power Current (I_{pm})	A	8.40
Short circuit current ($I_{s.c}$)	A	8.90
Maximum Power (P_{max})	W	250
Tolerance of P_{max}	%	+5/-0
PTC Rating	W	223.6
Dimensions	mm	994*1640*46
Weight	kg	19
NOCT	°c	47.5
Operating temperature	°c	-40 ~ + 90
Max Load	Pascal	2400
Module Efficiency	%	15.3

Source: SHARP (2018).

2.4.2. Wind Turbine Production

The wind turbine output power is affected by the hub height, air density and wind speed (Baneshi and Hadianfard, 2016). Figure 5 shows the output power of the proposed wind turbine. This study uses Xzeres AC wind turbine; its body is made of ductile iron casting and steel. Also, it has three phases neodymium permanent magnet alternator. Table 4 shows the technical specifications of the proposed wind turbine.

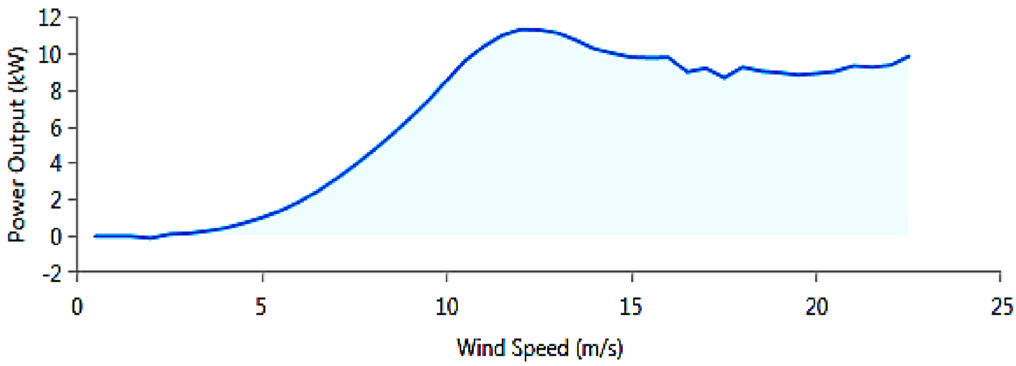

Figure-5. The power-speed curve of Xzeres 7.2 wind turbine.

Source: HOMER Pro software.

Table-4. Technical characteristics of the Xzeres 7.2 wind turbine.

Characteristics	Unit	Value
Rated power	kW	10
Cut-in wind speed	m/s	3.5
Swept Area	m^2	41
Rotor diameter	m	7.2
Hub height	m	24.40
Orientation	--	3-blade, upwind
Sound Level	dB	50.2
Lifetime	years	20

Source: xzeres (2018).

2.4.3. Diesel Generator

This paper uses a 50 kW fixed capacity generator as a backup power source. The generator has a minimum load ratio equals 25%. It consumes 1.65 Liter of diesel per hour. Table 5 illustrates the proposed generator gases emissions. The relation between the generator output power and its efficiency is shown in Figure 6 (HOMER Energy, 2018).

Table-5. Generic diesel generator gases emissions.

Description	Unit	Value
CO	g/L fuel	16.34
Unburned HC	g/L fuel	0.72
Particulates	g/L fuel	0.098
NOx	g/L fuel	15.359
Fuel Sulfur to PM	%	2.2

Source: HOMER Energy (2018).

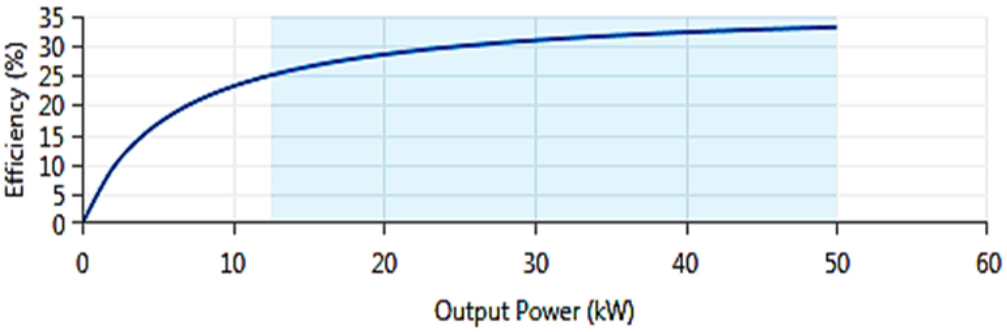

Figure-6. The power-efficiency curve of 50 kW Generic diesel generator.

Source: HOMER Pro software

2.4.4. Battery Bank

Trojan SAGM12 205 storage batteries are used to provide the load with the necessary electricity. The batteries are connected in series to produce high energy capacity. Table 6 shows the technical characteristics of the proposed storage battery.

Table-6. Technical characteristics of the Trojan SAGM 12 205 battery.

Characteristic	Unit	Value
Nominal voltage	V	12
Maximum capacity	Ah	219
Maximum charge current	A	41
Internal resistance	mΩ	4.5
Short circuit current	A	2790
Operating temperature	c	-20~+50
Lifetime	years	8+
Minimum state of charge	%	20
Dimensions	mm	380*176*357
weight	kg	59

Source: SOLAR TRUE DEEP-CYCLE AGM (2018).

2.4.5. Converter Sizing

Generic system converter is used for both rectification and inversion processes. It rectifies the wind turbine and diesel generator currents from AC to DC to store the excess electricity in the batteries. Also, it inverts the photovoltaic current from DC to AC to supply the load. The converter is connected in parallel with the generator. It has 15 lifetime years, and its efficiency equals 95%. In this simulation, the Homer optimizer selects the converter sizing.

2.5. Economic Analysis

Net present cost, cost of energy, real discount rate and project lifetime are essential parameters to select the optimal energy system configuration. Net present cost is the difference between the present value of income and payment during the project lifetime. It can be calculated by the following equation (Hossain *et al.*, 2017; HOMER Help Manual, 2018).

$$C_{NPC} = \frac{C_{tot}}{CRF(i,n)} \tag{2}$$

Where C_{tot} is the project lifetime total cost ($/year) which includes capital, operating, replacement, fuel, and maintenance cost. $CRF(i,n)$ is the capital recovery factor which can be calculated by the following formula (Isa *et al.*, 2016):

$$CRF(i,n) = \frac{i(1+i)^n}{(1+i)^n - 1} \tag{3}$$

Where n is the lifetime of the project. Also, i is the real discount rate which converts between the in-time and annualized costs. It can be expressed by the following formula (Hossain *et al.*, 2017; HHM, 2018).

$$i = \frac{i' - f}{1 + f} \tag{4}$$

Where i' is the nominal interest rate and f is the annual inflation rate.

Homer Pro software defines the cost of energy as the ratio between the total annualized cost ($/kWh) and the total served load. The following equation calculates the cost of energy (Hossain *et al.*, 2017; HHM, 2018).

$$COE = \frac{C_{tot}}{Load\ served} \tag{5}$$

in the above equation, C_{tot} is the project lifetime total cost ($/kWh) and load served is the RO desalination plant.

3. RESULTS AND DISCUSSION

This paper studied five different scenarios to operate an RO desalination plant at the Nakhl city, Egypt. The different scenarios are a stand-alone diesel generator system without a storage element, hybrid PV/diesel system with a storage element, hybrid wind/diesel system with a storage element, hybrid PV/wind system with a storage element and hybrid PV/wind/diesel system with a storage element. The results are obtained by comparing the net present cost, cost of energy, excess system electricity, gases emissions and the capacity shortage of the different scenarios. The optimal system configuration consists of 83.5 kW PV panels, a 50 kW diesel generator, seven strings of lead-acid batteries and a 36.4 kW converter.

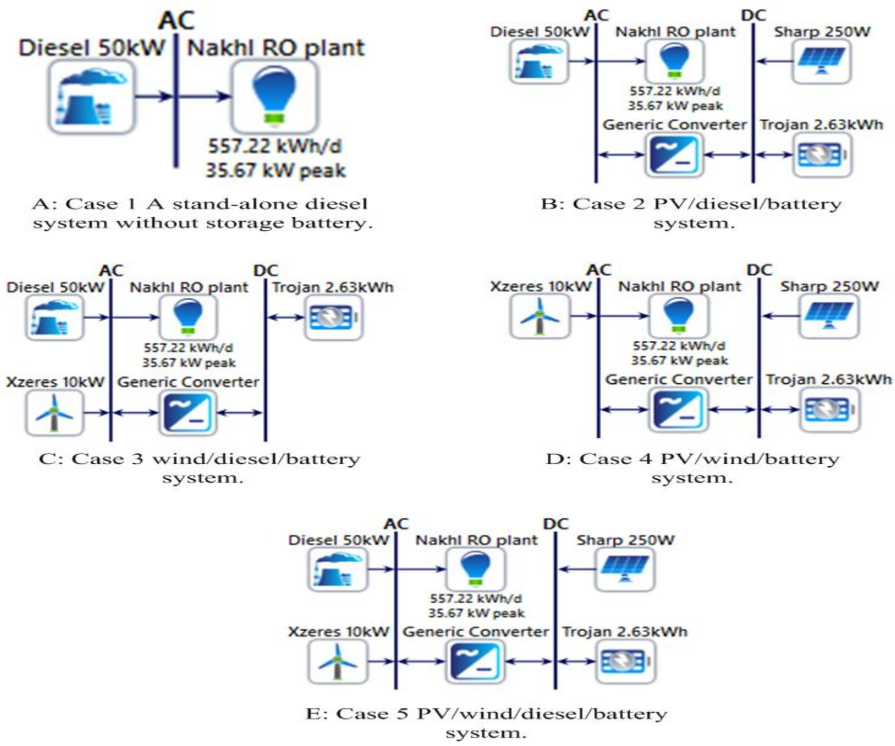

Figure-7. Different scenarios of off-grid hybrid RO desalination plant at Nakhl.
Source: Generated by the authors using HOMER Pro software

3.1. Case 1: A Stand-Alone Diesel Generator System without a Storage Element

The system configuration is shown in Figure 7A. This system ranks the 4th position between all cases. The diesel operates for 8,760 hours/year to produce 234,045 kWh of electricity per year. It consumes 78,348 liters of diesel annually. The total fuel cost equals $559,003.90 which represents about 46.57% of the net present cost as shown in Figure 8. The system releases a massive amount of CO_2 emissions which equals 205,106 kg/year. The system cost of energy and net present cost are $0.2564 and $1,200,435 respectively. The system produces 30,660 kWh/year of excess electricity which represents 13.1% of the total energy production. Fortunately, this electricity will be lost due to there is no storage element.

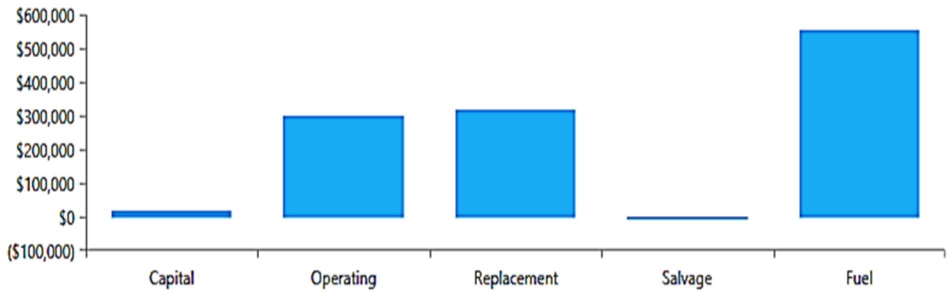

Figure-8. Cash flow summary of a stand-alone diesel system without storage battery.
Source: HOMER Pro software

3.2. Case 2: PV/Diesel/Battery System

The system configuration is shown in Figure 7B. It ranks the 1st position between all cases because it has the lowest net present cost and cost of energy which equal $725,536.70 and $0.1550 respectively. The diesel generator operates for 2,755 hours/year with mean electrical output power equals 32.5kW to produce 89,553 kWh of electricity per year which represents 37.4% of the total load. The generator consumes 28,994 Liters of diesel annually. The CO_2 emissions are reduced to 75,901 kG/year which equals 37% of CO_2 emissions in case 1. Also, 83.5 kW photovoltaic panels operate for 4,390hrs/year with mean output power equals 17.1kW to produce 150,060 kWh of electricity per year which represents 62.6% of the total load. Figure 9 illustrates the system monthly average production. The system produces 28,097 kWh of excess electricity per year which represents 11.7% of the total production. This electricity is stored in storage batteries to supply the load at night when no photovoltaic power. Seven strings of lead-acid batteries are connected in parallel. Figure 10 shows the batteries state of charge throughout the year. This system is characterized by zero capacity shortage and 56% renewable fraction.

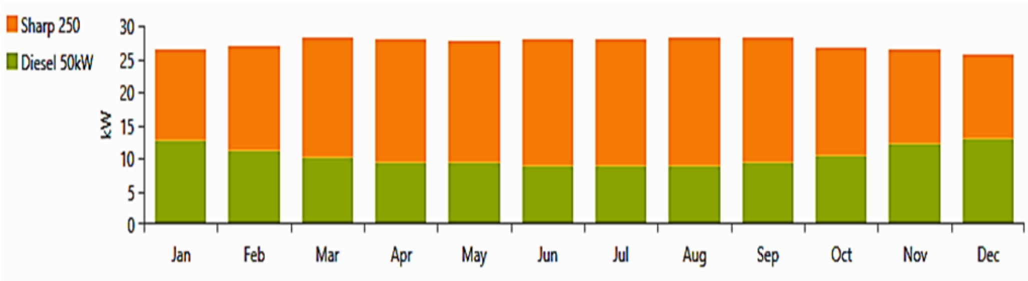

Figure-9. The optimal system monthly average electric production.
Source: HOMER Pro software

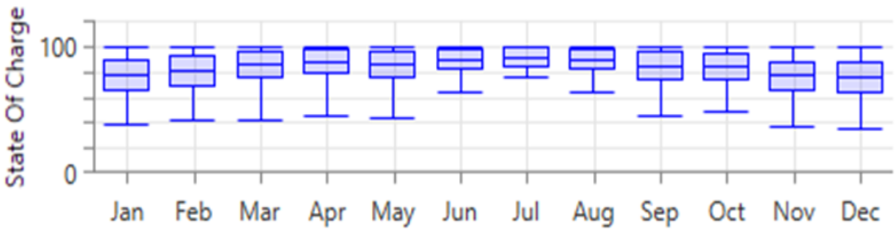

Figure-10. The batteries state of charge in the optimal case.
Source: HOMER Pro software

3.3. Case 3: Wind/Diesel/Battery System

The system configuration is shown in Figure 7C. It ranks the 3rd position between all cases. The diesel generator operates for 5,840hrs/year with mean electrical output power equals 33.5 kW to produce 195,756 kWh of electricity per year which represents 95.5% of the total load. The generator consumes 63,077 Liters of diesel per year and releases 165,128 kg/year of CO_2 emissions. Also, a 10.4 kW wind turbine operates for 6,924hrs/year with mean output power equals 1.06 kW to produce 9,327 kWh of electricity per year which represents 4.55% of the total production. Figure 11 illustrates the system monthly average electric production. Although the system produces 333 kWh of excess electricity per year, it has a low renewable fraction which equals 3.80%.

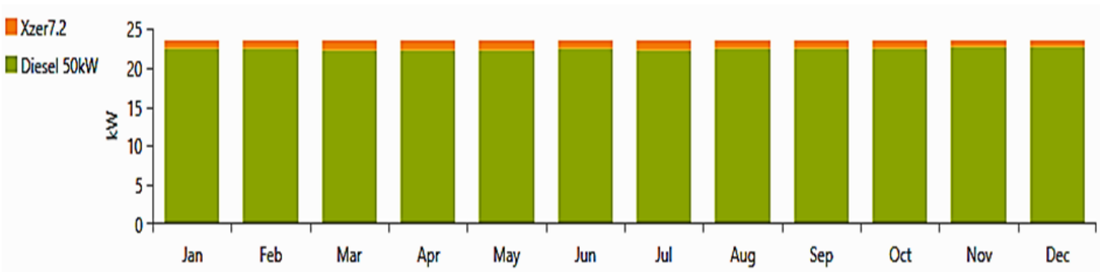

Figure-11. The monthly average electric production of the wind/diesel/battery system.
Source: HOMER Pro software

3.4. Case4: PV/Wind/Battery System

The system configuration is shown in Figure 7D. It ranks the last position between all cases due to its high cost. The photovoltaic system consists of 186 kW panels. They operate for 4,390 hours/year with mean output power 38.2kW to produce 334,249 kWh of electricity per year which represents 97.3% of the total production. Also, a 10 kW wind turbine operates for 6,924 hours/year with mean output power equals 1.06 kW to produce 9,327 kWh of electricity per year which represents 2.71% of the total production. Figure 12 shows the system monthly average electric production. There are 83 strings of lead-acid batteries are used to store the excess system electricity which equals 33.6% of the total production. The batteries cost are $807,632.85 which represents about 61% of the total cost. It means that much money is spent on the storage batteries only. Figure 13 illustrates the system cost summary. Although the system has zero gases emissions, it has 0.0528% of unmet electric load due to the capacity shortage which equals 0.0849%.

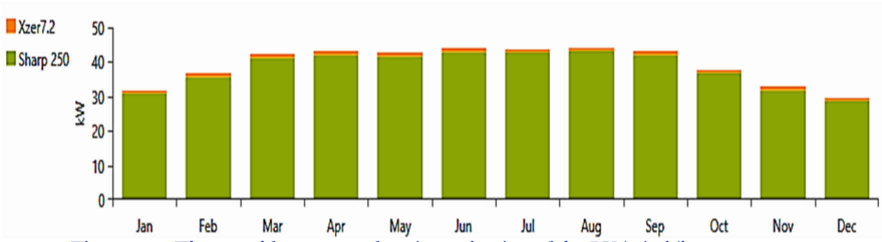

Figure-12. The monthly average electric production of the PV/wind/battery system.
Source: HOMER Pro software

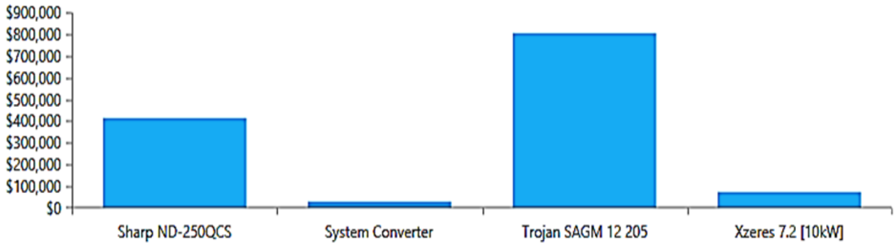

Figure-13. The cost summary of the PV/wind/battery system.
Source: HOMER Pro software

3.5. Case 5: PV/Wind/Diesel/Battery System

The system configuration is shown in Figure 7E. It tanks the 2nd position between all cases due to its low net present cost ($775,399.10) and high renewable fraction (57.9%). The diesel generator operates for 2,687hrs/year with mean electrical output power equals 31.9 kW to produce 85,713 kWh of electricity per year which represents 35.2% of the total production. The generator consumes 27,833 Liters of diesel per year and releases 72,863 kg/year of CO_2 emissions. Also, photovoltaic panels with 82.7 kW rated power operate for 4,390 hours/year with mean output power equals 17 kW to produce 148,628kWh of electricity per year which represents 61% of the total production. One wind turbine with 10kW rated power operates for 6,924hrs/year with mean output power equals 1.06kW to produce 9,327 kWh of electricity per year which represents 3.83% of the total production. Figure 14 illustrates the system monthly average electric production. This system produces 32,627 kWh/year of system excess electricity which represents 13.4% of the system production. Seven strings of lead-acid batteries are used to store the excess system electricity.

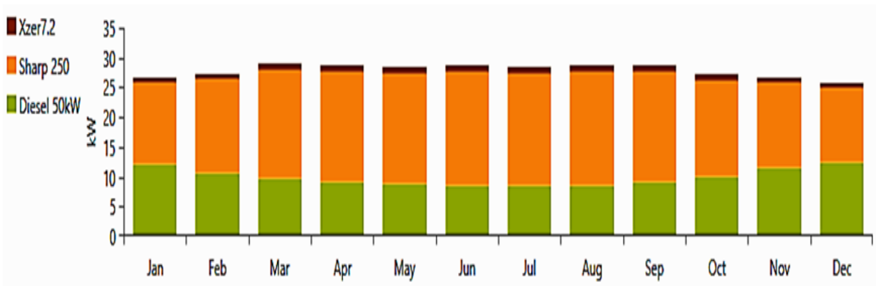

Figure-14. The monthly average electric production of the PV/wind/diesel/battery system.
Source: HOMER Pro software

Figure 15 shows the cash flow summary of the different cases. Figure 16 illustrates the value of CO_2 emissions in each case. Also, the cost of energy and net present cost for the different cases are illustrated in Figure 17.

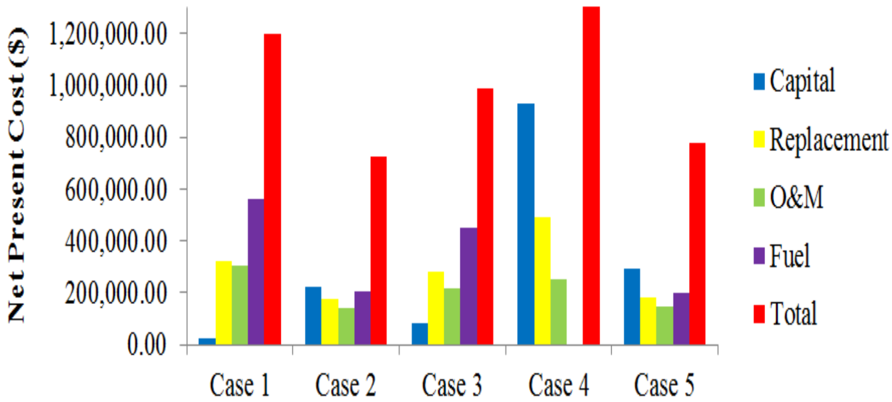

Figure-15. The cash flow summary of the different cases.

Source: Generated by the authors using HOMER Pro software data

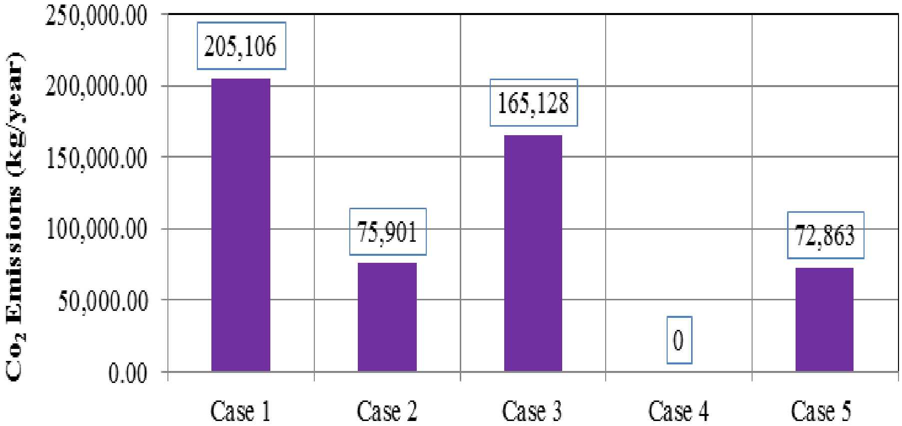

Figure-16. The value of carbon dioxide emissions in each case.

Source: Generated by the authors using HOMER Pro software data

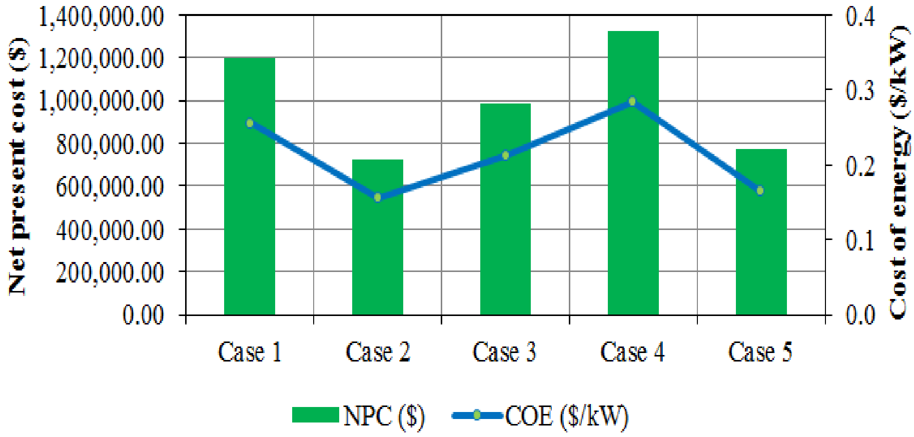

Figure-17. The Fnet present cost and cost of energy for all cases.

Source: Generated by the authors using HOMER Pro software data

4. CONCLUSION

Different scenarios for hybrid energy systems are studied to operate RO desalination plant at Nakhl city, Egypt. These scenarios consist of a stand-alone diesel generator system without a storage element, hybrid PV/diesel system with a storage element, hybrid wind/diesel system with a storage element, hybrid PV/wind system with a storage element and hybrid PV/wind/diesel system with a storage element. This study saves the potable water for 120,000 people at the peninsula of Sinai, Egypt. Homer Pro software simulated more than 500 solutions to select the optimal hybrid energy system design. This paper presents the five best solutions. After the accurate simulation, the following points are extracted from the study:

1. Case 2 presents the optimal hybrid energy system configuration.
2. The optimal hybrid system consists of PV panels, diesel generator, and storage batteries.
3. The storage batteries increase the system stability and reliability.
4. Renewable energy meets 62.6% of the total demand in case 2 which reduces CO_2 emissions.
5. The hybrid PV/diesel system with storage batteries achieves the lowest net present cost and cost of energy.
6. Case 4 fell to the last position because of its high net present cost and cost of energy.

Funding: This study received no specific financial support.
Competing Interests: The authors declare that they have no competing interests.
Contributors/Acknowledgement: The authors thankfully acknowledge the support and cooperation of the Electrical Power Engineering Department of Zagazig University for their great help.

REFERENCES

Ahmed, F.E., R. Hashaikeh and N. Hilal, 2019. Solar powered desalination–technology, energy and future outlook. Desalination, 453: 54-76.Available at: https://doi.org/10.1016/j.desal.2018.12.002.

Arribas, L., L. Cano, I. Cruz, M. Mata and E. Llobet, 2010. PV–wind hybrid system performance: A new approach and a case study. Renewable Energy, 35(1): 128-137.Available at: https://doi.org/10.1016/j.renene.2009.07.002.

Baneshi, M. and F. Hadianfard, 2016. Techno-economic feasibility of hybrid diesel/PV/wind/battery electricity generation systems for non-residential large electricity consumers under southern Iran climate conditions. Energy Conversion and Management, 100(127): 233-244.Available at: https://doi.org/10.1016/j.enconman.2016.09.008.

Bansal, R.C., F.Z. Ahmed and R.K. Saket, 2005. Some issues related to power generation using wind energy conversion systems: An overview. International Journal of Emerging Electric Power Systems, 3(2).Available at: https://doi.org/10.2202/1553-779x.1070.

CAPSELLS, 2018. Cleanarcpower. Solar lighting and power products. Available from https://www.capsells.com/products/xzeres-10kw-wind-turbine.html.

Daud, A. and M. Ismail, 2012. Design of isolated hybrid systems minimizing costs and pollutant emissions. Renewable Energy, 44: 215-224.Available at: https://doi.org/10.1016/j.renene.2012.01.011.

Demiroren, A. and U. Yilmaz, 2010. Analysis of change in electric energy cost with using renewable energy sources in Gökceada, Turkey: An island example. Renewable and Sustainable Energy Reviews, 14(1): 323-333.Available at: https://doi.org/10.1016/j.rser.2009.06.030.

Ghenai, C., A. Merabet, T. Salameh and E. Pigem, 2018. Grid-tied and stand-alone hybrid solar power system for desalination plant. Desalination, 435: 172-180.Available at: https://doi.org/10.1016/j.desal.2017.10.044.

Global Petrol Prices, 2019. Globalpetrolprice.Com. Available from http://www.globalpetrolprices.com/Egypt/diesel_prices/.

GoGreenSolar, 2018. Gogreensolar site.

Gökçek, M., 2018. Integration of hybrid power (wind-photovoltaic-diesel-battery) and seawater reverse osmosis systems for small-scale desalination applications. Desalination, 435: 210-220.Available at: https://doi.org/10.1016/j.desal.2017.07.006.

Haidar, A.M., P.N. John and M. Shawal, 2011. Optimal configuration assessment of renewable energy in Malaysia. Renewable Energy, 36(2): 881-888.Available at: https://doi.org/10.1016/j.renene.2010.07.024.

Harder, E. and J.M. Gibson, 2011. The costs and benefits of large-scale solar photovoltaic power production in Abu Dhabi, United Arab Emirates. Renewable Energy, 36(2): 789-796.Available at: https://doi.org/10.1016/j.renene.2010.08.006.

HOMER Energy, 2018. Hybrid optimization model for electric renewables. Available from https://homerenergy.com/index.html.

HOMER Help Manual, 2018. National renewable energy laboratory, US. Available from http://www.homerenergy.com/pdf/HOMERHelpManual.pdf.

Hossain, M., S. Mekhilef and L. Olatomiwa, 2017. Performance evaluation of a stand-alone PV-wind-diesel-battery hybrid system feasible for a large resort center in South China Sea, Malaysia. Sustainable Cities and Society, 28: 358-366.Available at: https://doi.org/10.1016/j.scs.2016.10.008.

Isa, N.M., H.S. Das, C.W. Tan, A. Yatim and K.Y. Lau, 2016. A techno-economic assessment of a combined heat and power photovoltaic/fuel cell/battery energy system in Malaysia hospital. Energy, 112(C): 75-90.Available at: https://doi.org/10.1016/j.energy.2016.06.056.

Li, C.-H., X.-J. Zhu, G.-Y. Cao, S. Sui and M.-R. Hu, 2009. Dynamic modeling and sizing optimization of stand-alone photovoltaic power systems using hybrid energy storage technology. Renewable Energy, 34(3): 815-826.Available at: https://doi.org/10.1016/j.renene.2008.04.018.

Malik, A., 2011. Assessment of the potential of renewables for Brunei Darussalam. Renewable and Sustainable Energy Reviews, 15(1): 427-437.Available at: https://doi.org/10.1016/j.rser.2010.08.014.

Mehdi, T., B. Jamel and R. Xavier, 2014. Water/energy management approaches of an autonomous water desalination unit fed by a hybrid (Photovoltaic-Wind) system. International Conference on Electrical Sciences and Technologies in Maghreb (CISTEM).

NASA, 2018. National aeronautics and space administrative. Surface meteorology and solar energy. Available from http://eosweb.larc.nasa.gov/sse/.

Nema, P., R. Nema and S. Rangnekar, 2009. A current and future state of art development of hybrid energy system using wind and PV-solar: A review. Renewable and Sustainable Energy Reviews, 13(8): 2096-2103.Available at: https://doi.org/10.1016/j.rser.2008.10.006.

Ngan, M.S. and C.W. Tan, 2012. Assessment of economic viability for PV/wind/diesel hybrid energy system in southern Peninsular Malaysia. Renewable and Sustainable Energy Reviews, 16(1): 634-647.Available at: https://doi.org/10.1016/j.rser.2011.08.028.

Phuangpornpitak, N. and S. Kumar, 2011. User acceptance of diesel/PV hybrid system in an island community. Renewable Energy, 36(1): 125-131.Available at: https://doi.org/10.1016/j.renene.2010.06.007.

SHARP, 2018. Sharp ND-250QCS. Sharp solar electricity. Japanese multinational corporation. Available from https://www.zonnepanelen.net/nl/pdf/panels/ND-250QCS.pdf.

SOLAR TRUE DEEP-CYCLE AGM, 2018. Solarpaneltalk. Available from https://www.trojanbattery.com/pdf/SAGM_12_205_AGM_DS.pdf.

SOLARIS, 2018. Solar energy supply store. Available from https://www.solaris-shop.com/compare/4034/4053/4054/4055.

Talaat, M., M. Farahat and M. Osman, 2016. Assessment of earthing system location for wind turbines using finite element method. Renewable Energy, 93: 412-423.Available at: https://doi.org/10.1016/j.renene.2016.03.001.

Trading Economics, 2018. Egypt interest rate. Available from www.aquicomm.com/assets/docs/UK-XZERES-Wind-Europe.pdf.

xzeres, 2018. Xzeres wind turbine, xzeres machines for serious power. Available from www.aquicomm.com/assets/docs/UK-XZERES-Wind-Europe.pdf.